DESIGN
2024

Design challenges in leveraging binder jetting technology to innovate the medical instrument field

Lorenzo Cocchi, Marco Mariani, Serena Graziosi ✉, Roberto Viganò and Nora Lecis

Politecnico di Milano, Italy

✉ serena.graziosi@polimi.it

Abstract

Despite its significant advantages in terms of design freedom and the wide range of processable materials, the Binder Jetting technology has not yet received substantial attention in the healthcare field, especially concerning the fabrication of metal components. Hence, the paper investigates how this technology could be exploited to innovate the medical instrument field. Based on selected case studies, some preliminary design indications are derived on how to properly consider the various phases (i.e., printing, depowdering, and sintering) and related challenges of the Binder Jetting process.

Keywords: additive manufacturing, biomedical design, binder jetting, design for additive manufacturing

1. Introduction

The healthcare system and the various fields of medicine are undergoing significant transformations promoted by the increasing digitalisation of processes. Among these significant transformations is the progressively widespread adoption of 3D printing technologies, even at the point of care (Thieringer et al., 2022), with 3D printing machines installed directly inside hospitals. This possibility has stimulated studies on exploiting these technologies' design and fabrication potential and managing the digital workflow linked to their use (Daoud et al., 2021) within the healthcare context and regulations. Areas of applications of 3D printing pertain to multiple aspects (Kumar et al., 2021): from the bio-printing of tissues to the fabrication of medical instruments, the creation of anatomical models for preoperative planning, the development of patient-specific implants, and the 3D printing of drugs, among others. In specific medical fields, such as cranio- and maxillofacial surgery, 3D printing has already become an integral part of the digital treatment received by the patient (Murtezani et al., 2022).

In such a broad context, the field of orthopaedic surgery stands out for being one of the early adopters of 3D printing technologies within the medical community (Rodriguez Colon et al., 2023), where applications include, among others, the development of patient-specific implants and surgical guides, where subtractive technologies make the development of personalised solutions economically unsustainable (Rodriguez Colon et al., 2023). These guides are designed to assist the surgeon in tasks such as implant positioning, especially in cases where an altered anatomical situation must be managed, thus improving the implant's placement (Rodriguez Colon et al., 2023).

Therefore, together with implants, the fabrication of 3D-printed medical instruments is also a relevant application field for Additive Manufacturing (AM), especially when unconventional solutions are needed, for example, in the case of minimally invasive surgical procedures or specific diseases (Culmone et al., 2019). Instruments can thus also be customised based on surgeons' needs (Culmone

et al., 2019). Introducing modifications in the instruments used by surgeons can bring ergonomic benefits and, more generally, reduce occupational hazards (Putnam et al., 2023). Indeed, surgeons frequently perform repetitive operations in inconvenient positions that involve significant forces and may promote the development of injuries (Putnam et al., 2023). 3D printing technologies could address these issues by supporting the development of tailored solutions (Putnam et al., 2023). Hence, there is potential for the application of AM to advance the field of surgical instrumentation by providing patient- and surgeon-specific solutions to expand the field of personalised medicine with positive impacts on the well-being of patients and healthcare professionals.

The study presented in this paper falls within this realm. In addition, as a further research contribution, the potential of the Binder Jetting (BJT) technology for this aim is investigated. Indeed, the potential of BJT in the biomedical field has not yet been fully explored, especially in the case of metals. The field's most used metal AM processes are Powder Bed Fusion (PBF) and Direct Energy Deposition (DED). This limitation is noteworthy, as BJT is the only system exploiting an indirect approach to process a dry particulate feedstock. The printing process generates the so-called "green part" by selectively binding a powder bed at a low temperature. This "green part", which is fragile, is then depowdered to remove the unprocessed material. The densification process is obtained later through sintering, as in Material Extrusion (MEX) with metal filaments (Shaikh et al., 2021) or as in Metal Injection Molding (MIM). The possibility of having complete control over the sintering process parameters (i.e., sintering temperature, heating rate, atmosphere type, and pressure) is beneficial because it expands the range of processable materials with the BJT and minimises the risk of defects and residual stresses that are, instead, common issues in PBF and DED. On the other hand, the powder bed enables almost unlimited design freedom because the powder supports the parts' geometry during printing, even hanging surfaces or protrusions. Besides, BJT allows the manufacturing of more cost-efficient solutions than metal PBF (Blunk and Seibel, 2023). Despite these advantages, BJT faces several critical issues, primarily related to powder bed packing density. This affects sintering mechanisms and final part properties, limiting the range of acceptable powder sizes and morphologies. Additionally, the geometrical resolution is constrained by powder-binder interactions and printhead features, whose resolution can be higher than laser- or light-induced consolidation processes, depending on the density, number, and size of the nozzles. Furthermore, the low initial green density leads to significant shrinkage, which is not isotropic (porosity is prevalent in the vertical direction). It may cause visible distortions due to multiple factors, even in the case of relatively simple geometries, as observed by Zago et al. (2022). Nonetheless, the dimensional reduction associated with shrinkage can simplify the production of finer details in the final component since the corresponding printed parts are larger. As already known by the powder metallurgy and ceramic industries, the components may be subjected to distortions induced by a series of factors such as inhomogeneous porosity distribution, gravity, friction with the substrate plate, onset of viscous deformation in case of liquid phase sintering, internal stresses generated by thermal gradient. A combination of counter-deformed designs and support structures is needed to prevent undesirable deformations leading to non-functional parts. However, despite these open challenges, examples of biomedical applications of BJT, albeit unrelated to surgical instruments, have already highlighted the flexibility of BJT. Indeed, customisation of drug delivery systems can be achieved, as Chen et al. (2022) discussed. Orthopaedic implant prototypes were produced entirely of porous ceramic scaffolds, such as hydroxyapatite (Zhou et al., 2020) or a biocompatible magnesium substrate coated with a ceramic film (Kuah et al., 2022). An example of a metal partial denture framework is described in Mostafaei et al. (2018) and Onler et al. (2022).

Hence, the aim of this study is twofold. The first is exploring an alternative production technology (i.e., BJT) to subtractive manufacturing for medical instrument design and fabrication. Any fabrication defects and, in general, inaccuracies that could negatively affect the device functionalities and, therefore, the correctness and the success of a surgical operation must be avoided. For this exploration, case studies were selected in collaboration with Adler Ortho® (www.adlerortho.com), a manufacturer of joint prostheses and orthopaedic surgical devices. These case studies were also used to fulfil the second aim of the work, which is contributing to extending the knowledge concerning the Design for AM (DfAM) possibilities offered by BJT, considering that design guidelines for this

DESIGN FOR ADDITIVE MANUFACTURING

technology are still limited (Blunk and Seibel, 2023). In this regard, evaluations on the development of parts from a geometrical standpoint should consider that multiple steps are required in BJT. Therefore, when designing for AM (DfAM), it is important to account for their cumulative effects.

2. Material and methods

As discussed, the study aims to explore the feasibility of using BJT to print orthopaedic surgical instruments and identify the main design and fabrication challenges. Dedicated samples (Figure 1) were designed and fabricated with the Desktop Metal Shop System 3D printer by Aidro srl (aidro.it). The maximum printing dimensions are 350 mm x 222 mm x (h)200 mm. The material selected for the study is precipitation hardening stainless steel 17-4PH, whose hardness is suitable for the surgical instruments considered in our study. The feedstock employed is a spherical powder produced by gas atomisation with a monomodal distribution featuring D10 = 10 μm, D50 = 25 μm and D90 = 50 μm. The samples were printed with a 75 μm layer thickness. After printing, the powder is cured at a low temperature, allowing for the consolidation of the green bodies through polymerisation of the water-based binder (SS-01 by Desktop Metal). Samples are first depowdered by manual brushing combined with compressed air blowing and then debinded to remove the organic ligand residue. Densification is obtained through a sintering treatment up to 1310°C in a slightly reducing atmosphere (97% Ar/3% H$_2$) to prevent the oxidation of the parts. All the components were placed on ceramic plates during the thermal treatments to avoid contamination or bonding with the substrate. The reasoning that has guided the design of the samples shown in Figure 1 is explained as follows.

Prismatic samples were printed to control the outcome and the reliability of the printing process. Three sets of prisms were produced (Figure 1A): series "S" (small), series "M" (medium), and series "L" (large). All prisms were oversized at the design stage by the following scale factors, i.e., 1.167 (x-axis), 1.174 (y-axis) and 1.21 (z-axis), to compensate for the linear shrinkage occurring during the densification at the sintering phase. These values were set based on the expertise of the machine operators. Samples were labelled through numbers (e.g., "1" in Figure 1A). Three replicas each were printed. The second type of sample (Figure 1B) was conceived to test the machine's resolution and identify potential differences along the x- and y-axes and to evaluate minimum dimensions concerning the three phases involved in the BJT process, i.e., printing, depowdering and sintering. This sample has 10 through holes, 10 cylinders and 10 walls whose dimensions vary from 0.1 to 1 mm with a discretisation of 0.1 mm (Figure 1B). The third type of sample (Figure 1C) was designed to test the influence of friction during the sintering process and to start evaluating the possibility of printing complex geometries. We selected, as a reference, a trial shell. This instrument is used in hip replacement surgery to support the reaming phase of the acetabulum. We modified the original geometry by introducing additional radial holes to reduce its weight, one of the expected targets for using AM in this field, and simultaneously to create a challenging geometry for the sintering phase. The shell was printed with the central axis parallel to the printing direction to avoid the formation of a non-uniform external surface owing to the stepwise effect typical of the layer-wise process.

An extract of the femoral broach represents the fourth sample (Figure 1D). This instrument is used in hip replacement surgery to prepare the femoral canal for the insertion of the hip system. This instrument is particularly challenging for BJT, considering the presence of knife edges. These edges are fundamental for the necessary digging operation to create the canal before the implant insertion. However, these knife edges are also features that should be avoided in BJT because they will likely not survive the debinding phase (Mostafaei et al., 2021). Besides, together with the presence of knife edges, this type of instrument presents challenges concerning its significant axial length, which poses reflections concerning the printing and the sintering orientations and the amount of space occupied by the component. As a starting point, we extracted a portion of the digital model of the instrument to generate the sample.
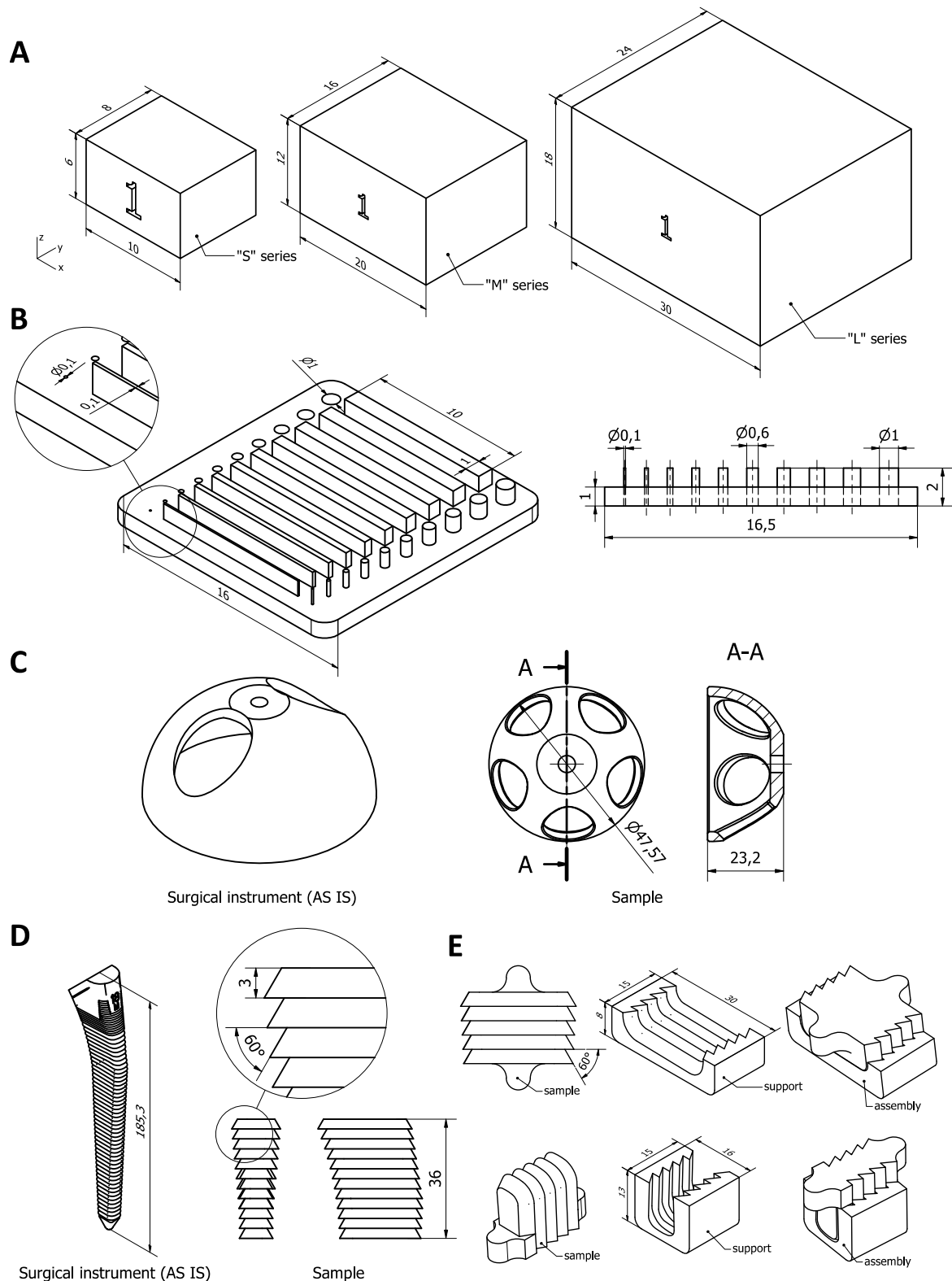
Figure 1. Overview of the samples used for the study: A) "S", "M", and "L" prisms; B) resolution sample, isometric (left) and lateral (right) views; C) how the geometry of a standard trial shell was converted into a sample; D) the femoral broach (left) and the sample used (right); E) samples with knife edges and related supports printed horizontally- (top) and vertically- (bottom) oriented. Linear dimensions are expressed in millimetres

The fifth class of samples was designed to deepen two research needs. The first was to create samples to test some finishing processes for the knife edges, with these oriented horizontally (Figure 1E, top) and vertically (Figure 1E, bottom). The geometry of this sample has been designed to allow the selected finishing machine to operate on it. However, it is worth clarifying that these finishing aspects are not the focus of this paper. Hence, they will not be further discussed. The aspects discussed here are related to the design of the supports for the sintering phases. Indeed, the use of support in BJT is an aspect that is rarely discussed in the literature. Supports are not needed during printing; instead, they could be necessary to accommodate deformations occurring during the sintering phase. How to design them and what considerations should be made to leverage them properly are topics not fully clarified in the literature. To this aim, the samples in Figure 1E were designed. It is also worth highlighting that samples for characterising material properties were also printed and tested. However, these details are not part of this work, which focuses on deriving preliminary insights concerning the printability of specific features and shapes.

The dimensions of the printed prims were evaluated by multiple measurements along the three axes by a digital calliper. Their sintered density was measured both by geometrical and Archimedes' methods for prisms "S" and "M" (Figure 1A) and by the geometrical method alone for prisms "L" (Figure 1A) due to dimensional limitations of the Archimedes' scale. Their relative density was calculated by considering a theoretical full density equal to $7.80 \, \mathrm{g \cdot cm^{-3}}$. For the prims, the distribution of the residual porosity was observed by light optical microscopy (LOM) on polished cross-sections along the perpendicular (XY plane) and parallel (XZ) surfaces with respect to the building direction (Z). Visual inspections and measurements through a digital calliper and 3D scanning (FARO Arm Quantum Max) were performed for the other samples.

3. Results and discussion

The printed, debinded, and sintered prims (Figure 1A) are shown in Figure 2A, their micrographs in Figure 2B, and their geometrical and density measurements are presented in Table 1.
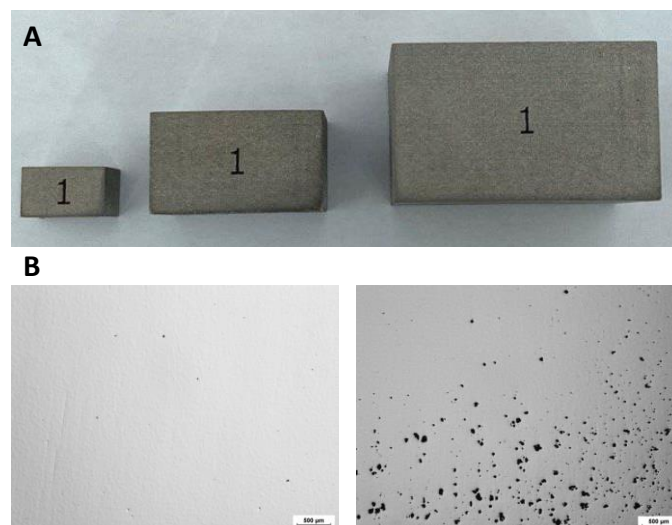
Figure 2. The prisms (A) and micrographs of the XZ (B, left) and XY (B, right) planes cross sections obtained by LOM

The final size along the three axes was superior in all cases, except for the Z value of the "L" prism, highlighting that the assigned oversizing exceeded the linear shrinkage during sintering. The "L" series suffered minimal discrepancy with respect to the desired final dimension; nonetheless, the standard deviation values were higher in this case. Thus, the repeatability and accuracy of the printing process slightly deteriorated for larger volumes.

Geometrical density values (Table 1) display a positive trend with increasing dimensions, up to 97% for the "L" prisms. Archimedes' density (Table 1) confirms such behaviour; however, the difference among the "S" and "M" series is reduced compared to the precedent values. This might be due to the improved

accuracy of Archimedes' technique, which is less influenced by the surface roughness and independent of the actual shape of the components; they might be slightly distorted with respect to the ideal prism. Overall, it can be concluded that low surface-to-volume ratios are beneficial for the densification (i.e., the sintering) process. However, in all cases, the sintering was achieved coherently with previous results on 17-4PH presented by (Huber et al., 2021). Micrographs in Figure 2B confirm the progress of densification and highlight that residual pores are primarily spherical, closed, and isolated. In addition, in the XY section, the porosity is not homogeneously distributed but instead concentrated at the interlayer regions crossed during polishing, as explained by Cabo Rios et al. (2022).

Table 1. Average size, mass and relative density values measured for the prismatic samples; Their theoretical dimensional values are available in Figure 1A

| Prisms series	S	M	L
X [mm]	10.17 ± 0.01	20.18 ± 0.03	30.15 ± 0.04
Y [mm]	8.13 ± 0.03	16.09 ± 0.04	24.07 ± 0.09
Z [mm]	6.16 ± 0.03	12.06 ± 0.02	17.99 ± 0.05
Mass [g]	3.74 ± 0.02	29.44 ± 0.09	98.98 ± 0.67
$\rho rel,geom$ [%]	94.03 ± 0.40	96.28 ± 0.31	97.02 ± 0.15
$\rho rel,arch$ [%]	96.71 ± 0.62	97.15 ± 0.08	/

Figure 3 shows the resolution capabilities of the printer. Built parts provide contradictory results: rectangular walls could be produced and maintained throughout the process down to a thickness of 0.2 mm (the 0.1 mm thickness was almost complete); on the contrary, only isolated cylinders with a minimum diameter of 0.7 mm could reach the final stage intact. Through-holes could be added in the green body, but internal diameters inferior to 0.5 mm could not be entirely depowdered.

In addition to the resolution limitations associated with the printhead and its nozzle features, other aspects and procedures might affect the outcome. The depowdering procedure, which is performed on the "green" part after the printing, can be detrimental to the quality of the printed parts due to the severe stresses applied to the green body that typically features minimal mechanical strength; thus, finer details might be demolished during the extraction of the components from the loose powder after curing. This is a critical issue for parts with a high surface-to-volume ratio (e.g., the cylinders), whose resistance to shear and bending is limited.

Ø 0.5 mm (hole) limit for depowdering

Ø 0.7 mm limit for depowdering

0.1 mm wall thickness
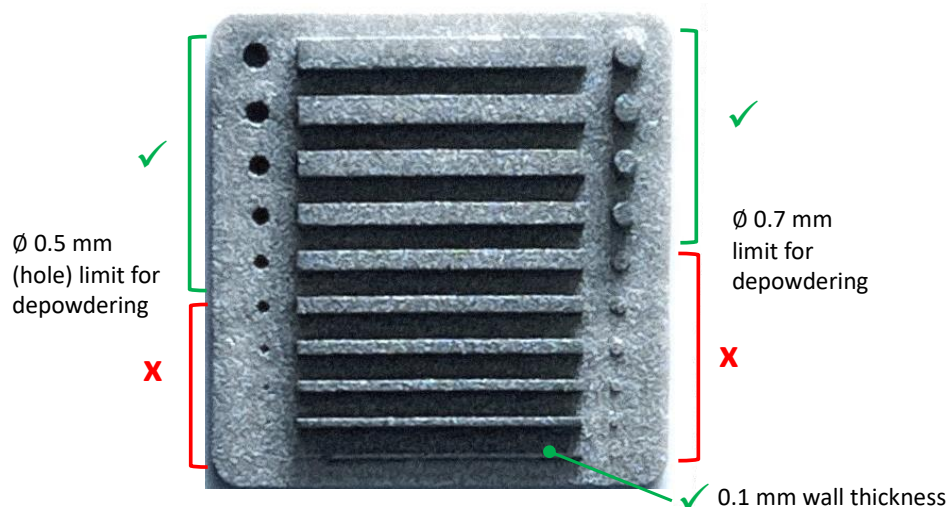
Figure 3. The printed and sintered resolution sample (see also Figure 1B)

Regarding channels and cavities, the resolution is also limited by the infiltration behaviour of the binder. The liquid spreads laterally upon deposition on the bed surface and wets out-of-bounds particles; thus, droplets deposited on the internal surface of the smaller holes might coalesce, leading to its closure by completely wetting the particles within the channel.

Figure 4 shows the difference between samples of the trial shell (Figure 1C) printed in the same manner (upward cavity) and sintered with opposite placements. It can be observed that the specimen sintered with the downward cavity displays two cracks, while the second sample is still intact. Both have suffered from excessive distortions, although partial compensations were added during the design phase.
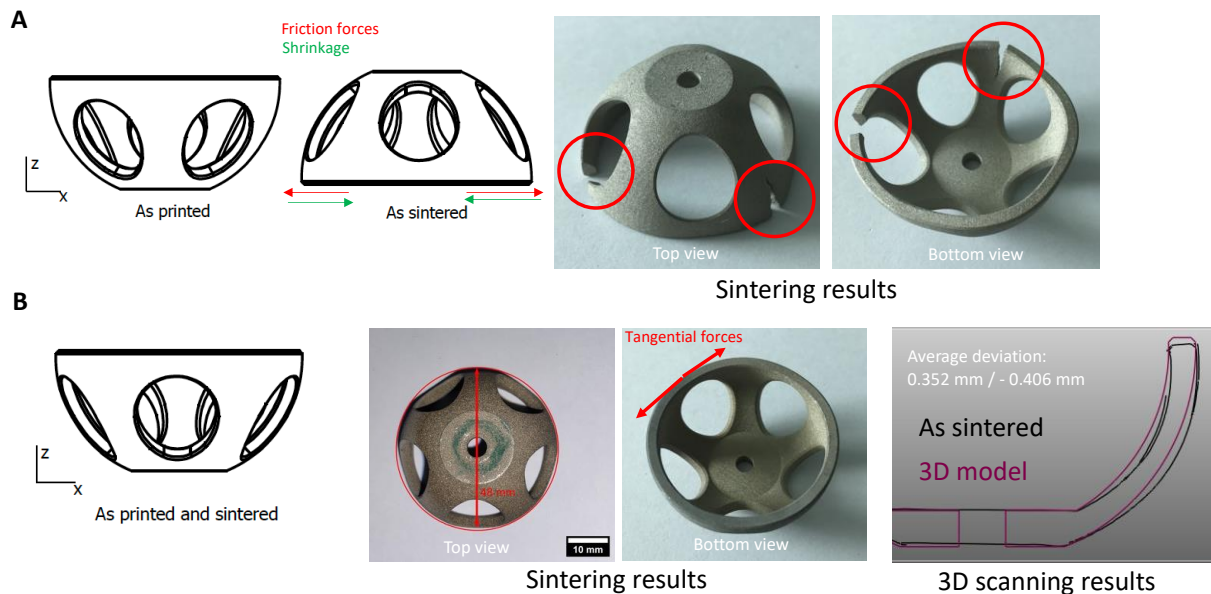

Figure 4. The trial shell results: A) Cracks visible after sintering a trial shell with the cavity oriented downward; B) Results obtained by sintering the trial shell with the cavity oriented upward; No cracks are visible, but the sample is distorted

Regarding the shell in Figure 4A, cracks developed between and in correspondence of the holes. Such defects result from internal stresses developed due to densification acting on a constrained structure. Indeed, the relevant linear shrinkage, especially in the horizontal directions, would induce the motion of all surfaces toward the shell's core along the radial direction. However, the bottom surface is subject to friction with the ceramic plate; thus, this region is a constraint. In addition, the stresses developed along the tangential direction due to the inhomogeneous distribution of material within the structure. Holes remove weight as well as pulling forces from the bottom surfaces, while connection brackets act in the exact opposite manner: they generate a pulling stress with components directed both radially and tangentially; at the same time, they add mass above the base, thus pinning it locally due to friction. As a result, the intact half of the shell deformed, generating a flat side due to unconstrained shrinkage below the hole, while the other half broke due to excessive build-up of internal stresses.

The intact shell in Figure 4B demonstrates that properly planning the sintering procedure is necessary and beneficial. Indeed, severe deformations and cracks are not present; thus, the part's integrity is guaranteed. Nonetheless, undesired distortions are still detected (e.g. the base is no longer a circle; see Figure 4B vs Figure 1C), especially due to uneven mass distribution among brackets and holes; on one hand, the inhomogeneous shrinkage in the radial direction worsened the circularity of the upper surface; on the other hand, the gravity acting on the additional weight and the pulling force due to densification led to excessive collapse of the shell in the vertical direction.

Figure 5 shows the results of the sintering procedure on a section of a femoral broach (Figure 1D), which was printed vertically. Due to the high height-to-base ratio, the part must be placed with the main axis in the horizontal direction; otherwise, the structure would be too unstable, and its physical transfer from the printer to the furnace would be impractical. However, such orientation led to a visible distortion along its length: the structure tends to bend due to gravity, producing a visible flattening of the surface

in contact with the plate. In addition, the sharp edges deteriorate, thus providing unsatisfactory accuracies on the bottom half of the component.
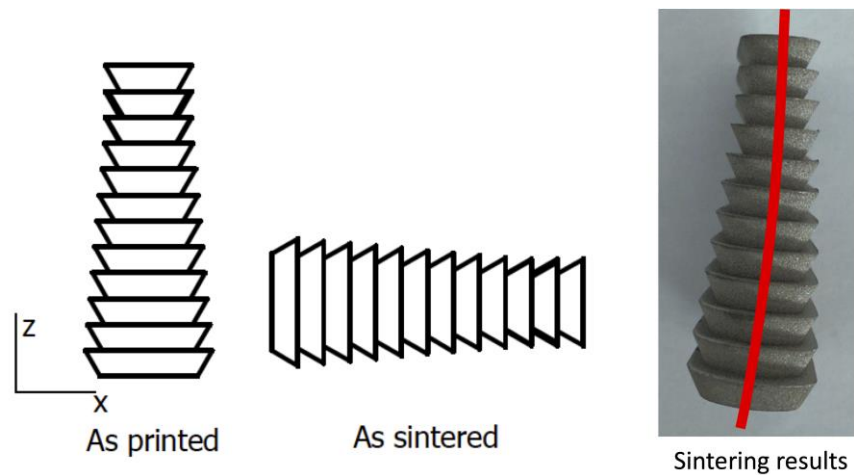
Figure 5. The sintering results of the femoral broach

Finally, Figure 6 shows the results of supported and unsupported sintering on half sections of broaches. From the result mentioned above, the presence of the supports was revealed to be necessary. Still, it should be considered that these structures are equally subject to all mechanisms described in the previous cases. So, reciprocal influence from and on the supporting components must also be considered.
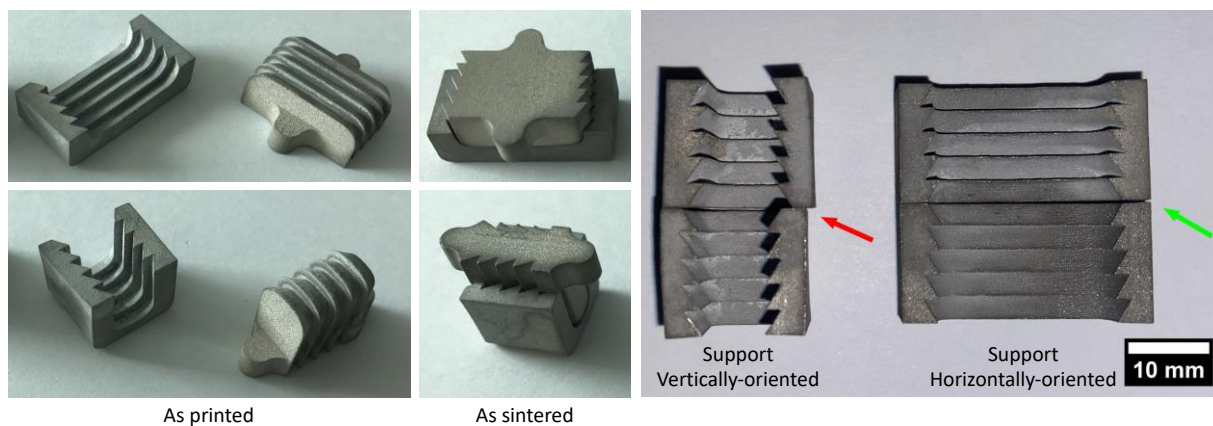
Figure 6. The results of the samples printed with the supports; On the right, the arrows indicate that the vertically oriented support underwent distortions due to its low height-to-base ratio alongside its vertical walls compared to the horizontally-oriented ones

First, it should be noted that shape retention was significantly improved for both components, regardless of the aspect ratio, and the broaches sections did not bend. Both broaches and supports get densified and shrunk as expected. However, distortions can still be found, especially in the sample with a low height-to-base ratio alongside its vertical walls and in its support (Figure 6, right). Vertical walls with high height-to-thickness ratios are prone to bending, or worse collapse, on one side (Blunk and Seibel, 2023). In our case, supports suffered from such a defect, and the presence of the part itself prevented further distortion. Therefore, it can be inferred that shrinking supports, or parts of them, may develop pressure on the supported component, thus altering the densification behaviour. This may be detrimental to the reproducibility of the process if the support distortion cannot be controlled or if its shrinkage is not homogeneous within its volume.

4. Conclusions

The work presents a preliminary investigation of the feasibility of leveraging the BJT technology as a potential manufacturing technology to innovate the field of orthopaedic metal surgical instruments.

Considerations were derived based on the experience gathered on selected samples used as case studies. These samples were designed to deepen the phenomena occurring at the different stages of the BJT manufacturing process, not limited to the printing phase but also the depowdering and sintering ones. To this aim, these samples were printed, debinded and sintered, and the following insights were derived from the analysis of the obtained results:

- Densification leads to severe and different linear shrinkage values along the X, Y and Z axes, with a clear dependence on the deposition direction of the powder layers and the binder droplets.
- Resolution is dependent primarily on the printhead features and capabilities. Still, the possibility of producing thin features also correlates to the risk of detachment and failures during depowdering operations that significantly stress the green bodies.
- Parts with asymmetric mass distributions should be placed in the sintering furnace according to the internal stresses that could develop during sintering due to uneven shrinkage, gravity-induced deformation and differential friction forces generated among the bottom surface and the support plates.
- The use of 3D-printed supports is needed for complex geometries to prevent distortions and flattening by eliminating or controlling the occurrence of the previous mechanisms, although supports themselves could be affected by such phenomena.
- The design of these supports should be studied to determine how to optimise them for homogeneous parts densification and shrinkage while accounting for weight (thus cost) minimisation.

From the printing point of view, no significant issues have been identified, even in the case of massive geometries that could be challenging to print with other AM technologies, demonstrating the printing potential of BJT in the manufacturing of metal components. However, different from other metal AM technologies, at the design stage of components for BJT, aspects related to the debinding and sintering phases must also be considered to avoid breakage and distortion after printing. Further investigations are needed to deepen these aspects, particularly how they influence the design and functionalities of surgical instruments in combination with mechanical properties and finishing-related considerations.

Acknowledgements

References

Blunk, H. and Seibel, A. (2023), "Design guidelines for metal binder jetting", *Progress in Additive Manufacturing*, https://dx.doi.org/10.1007/s40964-023-00475-y.

Cabo Rios, A., Hryha, E., Olevsky, E. and Harlin, P. (2022), "Sintering anisotropy of binder jetted 316L stainless steel: part II – microstructure evolution during sintering", *Powder Metallurgy*, Vol. 65 No. 4, pp. 283–295, https://dx.doi.org/10.1080/00325899.2021.2020486.

Chen, X., Wang, S., Wu, J., Duan, S., Wang, X., Hong, X., Han, X., *et al.* (2022), "The Application and Challenge of Binder Jet 3D Printing Technology in Pharmaceutical Manufacturing", *Pharmaceutics*, Vol. 14 No. 12, p. 2589, https://dx.doi.org/10.3390/pharmaceutics14122589.

Culmone, C., Smit, G. and Breedveld, P. (2019), "Additive manufacturing of medical instruments: A state-of-the-art review", *Additive Manufacturing*, Vol. 27, pp. 461–473, https://dx.doi.org/10.1016/j.addma.2019.03.015.

Daoud, G.E., Pezzutti, D.L., Dolatowski, C.J., Carrau, R.L., Pancake, M., Herderick, E. and VanKoevering, K.K. (2021), "Establishing a point-of-care additive manufacturing workflow for clinical use", *Journal of Materials Research*, Vol. 36 No. 19, pp. 3761–3780, https://dx.doi.org/10.1557/s43578-021-00270-x.

Huber, D., Vogel, L. and Fischer, A. (2021), "The effects of sintering temperature and hold time on densification, mechanical properties and microstructural characteristics of binder jet 3D printed 17-4 PH stainless steel", *Additive Manufacturing*, Vol. 46, p. 102114, https://dx.doi.org/10.1016/j.addma.2021.102114.

Kuah, K.X., Salehi, M., Huang, Z., Zhang, S.X., Seet, H.L., Nai, M.L.S. and Blackwood, D.J. (2022), "Surface Modification with Phosphate and Hydroxyapatite of Porous Magnesium Scaffolds Fabricated by Binder Jet Additive Manufacturing", *Crystals*, Vol. 12 No. 12, 1850, https://dx.doi.org/10.3390/cryst12121850.

Kumar, R., Kumar, M. and Chohan, J.S. (2021), "The role of additive manufacturing for biomedical applications: A critical review", *Journal of Manufacturing Processes*, Vol. 64, pp. 828–850, https://dx.doi.org/10.1016/j.jmapro.2021.02.022.

Mostafaei, A., Elliott, A.M., Barnes, J.E., Li, F., Tan, W., Cramer, C.L., Nandwana, P., *et al.* (2021), "Binder jet 3D printing—Process parameters, materials, properties, modeling, and challenges", *Progress in Materials Science*, Vol. 119, p. 100707, https://dx.doi.org/10.1016/j.pmatsci.2020.100707.

Mostafaei, A., Stevens, E.L., Ference, J.J., Schmidt, D.E. and Chmielus, M. (2018), "Binder jetting of a complex-shaped metal partial denture framework", *Additive Manufacturing*, Vol. 21, pp. 63–68, https://dx.doi.org/10.1016/j.addma.2018.02.014.

Murtezani, I., Sharma, N. and Thieringer, F.M. (2022), "Medical 3D printing with a focus on Point-of-Care in Cranio- and Maxillofacial Surgery. A systematic review of literature", *Annals of 3D Printed Medicine*, Vol. 6, p. 100059, https://dx.doi.org/10.1016/j.stlm.2022.100059.

Onler, R., Koca, A.S., Kirim, B. and Soylemez, E. (2022), "Multi-objective optimization of binder jet additive manufacturing of Co-Cr-Mo using machine learning", *The International Journal of Advanced Manufacturing Technology*, Vol. 119 No. 1–2, pp. 1091–1108, https://dx.doi.org/10.1007/s00170-021-08183-z.

Putnam, J.G., Kerkhof, F.D., Shah, K.N., Richards, A.W. and Ladd, A. (2023), "Helping Surgeons' Hands: A Biomechanical Evaluation of Ergonomic Instruments", *The Journal of Hand Surgery*, https://dx.doi.org/10.1016/j.jhsa.2022.12.006.

Rodriguez Colon, R., Nayak, V.V., Parente, P.E.L., Leucht, P., Tovar, N., Lin, C.C., Rezzadeh, K., *et al.* (2023), "The presence of 3D printing in orthopedics: A clinical and material review", *Journal of Orthopaedic Research*, Vol. 41 No. 3, pp. 601–613, https://dx.doi.org/10.1002/jor.25388.

Shaikh, M.Q., Graziosi, S. and Atre, S.V. (2021), "Supportless printing of lattice structures by metal fused filament fabrication (MF [3]) of Ti-6Al-4V: design and analysis", *Rapid Prototyping Journal*, Vol. 27 No. 7, pp. 1408–1422, https://dx.doi.org/10.1108/RPJ-01-2021-0015.

Thieringer, F.M., Honigmann, P. and Sharma, N. (2022), "Medical Additive Manufacturing in Surgery: Translating Innovation to the Point of Care", pp. 359–376, https://dx.doi.org/10.1007/978-3-030-99838-7_20.

Zago, M., Lecis, N., Mariani, M. and Cristofolini, I. (2022), "Analysis of the Flatness Form Error in Binder Jetting Process as Affected by the Inclination Angle", *Metals*, Vol. 12 No. 3, 430, https://dx.doi.org/10.3390/met12030430.

Zhou, Z., Lennon, A., Buchanan, F., McCarthy, H.O. and Dunne, N. (2020), "Binder jetting additive manufacturing of hydroxyapatite powders: Effects of adhesives on geometrical accuracy and green compressive strength", *Additive Manufacturing*, Vol. 36, p. 101645, https://dx.doi.org/10.1016/j.addma.2020.101645.